ISSN 1063-7761, Journal of Experimental and Theoretical Physics, 2013, Vol. 116, No. 5, pp. 860–865. © Pleiades Publishing, Inc., 2013.
Original Russian Text © E.N. Tkachev, T.I. Buryakov, V.L. Kuznetsov, S.I. Moseenkov, I.N. Mazov, S.I. Popkov, K.A. Shaikhutdinov, 2013, published in Zhurnal Eksperimental'noi i Teoreticheskoi Fiziki, 2013, Vol. 143, No. 5, pp. 991–997.

ELECTRONIC PROPERTIES OF SOLID

Current-Conducting Properties of Paper Consisting of Multiwall Carbon Nanotubes[1]

E. N. Tkachev[a,*], T. I. Buryakov[b], V. L. Kuznetsov[c], S. I. Moseenkov[c], I. N. Mazov[c], S. I. Popkov[d], and K. A. Shaikhutdinov[d]

[a] *Nikolaev Institute of Inorganic Chemistry, Siberian Branch, Russian Academy of Sciences, Novosibirsk, 630090 Russia*
**e-mail: etkachev@niic.nsc.ru*
[b] *Siberian Physicotechnical Institute, Tomsk State University, Novosobornaya pl. 1, Tomsk, 634050 Russia*
[c] *Boreskov Institute of Catalysis, Siberian Branch, Russian Academy of Sciences, Novosibirsk, 630090 Russia*
[d] *Kirensky Institute of Physics, Siberian Branch, Russian Academy of Sciences, Krasnoyarsk, 660036 Russia*

Abstract—Electrical conductivity $\sigma(T)$ of the paper consisting of multiwalled carbon nanotubes (MWCNTs) is studied in the temperature range 4.2–295 K, and its magnetoresistivity $\rho(B)$ at various temperatures in magnetic fields up to 9 T is analyzed. The temperature dependence of the paper electrical conductivity $\sigma(T)$ exhibits two-dimensional quantum corrections to the conductivity below 10 K. The dependences of negative magnetoresistivity $\rho(B)$ measured at various temperatures are used to estimate the wavefunction phase breakdown length L_φ of conduction electrons and to obtain the temperature dependence $L_\varphi = \text{const}\, T^{-p/2}$, where $p \approx 1/3$. Similar dependences of electrical conductivity $\sigma(T)$, magnetoresistivity $\rho(B)$, and phase breakdown length $L_\varphi(T)$ are detected for the initial MWCNTs used to prepare the paper.

DOI: 10.1134/S1063776113050257

1. INTRODUCTION

Composite materials based on carbon nanotubes are most promising for the applications using their properties [1]. The designing and properties of such materials are being extensively studied for various fields of application. Many works deal with the changes in the properties of composite materials that are caused by the introduction of a relatively low nanotube concentration [2, 3]. However, the properties of composite materials based on nanotubes with a low binder content have received little attention. Paper consisting of multiwalled carbon nanotubes (MWCNTs) with a low content or without a binder combines the unique properties of the initial nanotubes and the properties of a bulk material (film). Therefore, paper is a more convenient material for applied purposes as compared to the initial carbon nanotubes. Paper can be applied for catalysis, for ultrafiltration, in supercapacitors, as electrodes, for heat removal, and so on. One of the unique properties of carbon nanotubes and paper based on them is a high electrical and thermal conductivity. Nevertheless, the problems related to the electron transport in paper are still poorly understood. There are no systematic investigations of the electron transport in the paper consisting of MWCNTs with a controlled diameter distribution of carbon nanotubes, since the nanotube diameter and the presence of impurities and other carbon phases were not controlled [4–7]. In this work, we studied the electrophysical properties of the paper consisting of MWCNTs with a rather narrow diameter distribution of carbon nanotubes and revealed differences in the electron transport in the initial MWCNTs and the paper based on them.

2. EXPERIMENTAL

To prepare carbon nanopaper, we used carbon nanotubes with an average diameter of (20–22) ± 8 nm produced by catalytic decomposition of ethylene on an FeCo catalyst at 680–700°C. This type of catalyst and the chosen synthesis conditions ensured the formation of nanotubes with a narrow diameter distribution and a low content of impurities of other carbon forms. The prepared MWCNTs were cleaned from catalyst impurities by boiling in 15% hydrochloric acid for 3 h and were washed out in distilled water to achieve neutral pH (diameter distribution of nanotubes is shown in the inset to Fig. 1a). The average MWCNT diameter was measured upon statistical analysis of electron-microscopic images (400–500 individual MWCNTs).

To form MWCNT-based paper, we placed an MWCNT sample in a water-cooled reactor (Fig. 1b), poured 50 mL deionized water, and performed ultrasonic treatment for 30 min. Polyvinyl alcohol was used as a surfactant to improve the dispersive ability of carbon nanotubes and to form a stable suspension. After

[1] The article is based on a preliminary report delivered at the 36th Conference on Low-Temperature Physics (St. Petersburg, July 2–6, 2012).

ultrasonic treatment, the formed suspension was filtered through a fluoroplastic membrane (hole diameter of 0.45 μm) with a water-jet pump. The dense deposit formed on the filter was washed with hot water and acetone to remove the polyvinyl alcohol residue and was then dried in air.

The initial MWCNT samples represented loose powders. To measure the electrical resistivity, we pressed the powders into 2 × 10-mm glass cylinders. The contacts to a sample were made of 0.1-mm-thick silver wire pressed against it. To ensure contact between the sample and the wire, the powder was pressed through the end face of the glass cylinder until the electrical resistivity of the sample became almost constant upon an increase in the degree of compression (no more than 100 atm). This technique of measuring the electrical conductivity raises the question of the contact resistance between powder granules or nanotubes in the case of a material made of nanotubes. Of course, our technique cannot be used to obtain the electrical conductivity of the material, since the sample configuration used in this work is characterized by a current line distribution that differs from that in a single-crystal sample and the classical four-probe method of its measurement. The electrical conductivity in our case depends on the degree of powder compression at the end faces of the glass cylinder. Nevertheless, using such measurements, we can trace the change in the electrical conductivity induced by a change in the temperature, the magnetic field, and the characteristics of the material (imperfection, doping, etc.). Let us perform simple estimations and considerations to show that the objects (nanotubes) rather than contacts between them mainly contribute to the electrical resistivity to be measured. The electrical resistivity of quasi-two-dimensional graphite and MWCNTs is anisotropic. The anisotropy of nanotubes is $\rho_c/\rho_{ab} = 100$. The nanotube spacing cannot be smaller than the interlayer distance (0.344 nm); therefore, the contact length for estimation is taken to be $r = 0.35$ nm. The contact area is assumed to be $s = 10$ nm^2. The characteristics of MWCNTs are as follows: the outside diameter is 20 nm, the inside diameter is 10 nm, and the length is $L = 1000$ nm. Then, the nanotube cross-sectional area is $S \approx 30$ nm^2 provided a current passes through five external layers. The ratio of the contact resistance to the total nanotube resistance is

$$R_{\text{cont}}/R_{\text{tube}} = \frac{\rho_c}{\rho_{ab}}\frac{r}{L}\frac{S}{s} \approx 0.1;$$

that is, the contribution of the contact to the total resistance is at most 10%.

This result agrees with the results from other works. The authors of [8] used the four-probe method to study the resistance between the layers in MWCNTs and found that it is approximately 10 kΩ/μm, which is supported by numerical calculations of electron transitions between the neighboring π orbitals of two layers. The interlayer resistance is temperature-independent and is determined only by electron tunneling between the π orbitals of neighboring layers. As for the resistance of individual MWCNTs, the resistances measured in the first works dealing with this problem were significantly different and high (10–1000 MΩ) [9–12]. These results are likely to be related to bad contact with nanotubes because of the imperfect measurement technique used in those works. In [13, 14], electrodes were in contact with the internal layers of nanotubes: the better the contact, the lower the measured resistance (~1 kΩ). The resistance measured in [15, 16] was very low, about 10 Ω. In our technique of measuring the electrical resistivity (pressing of a material in a glass cylinder), the contacts between nanotubes were provided by only their surface layers. Therefore, the measurement techniques described

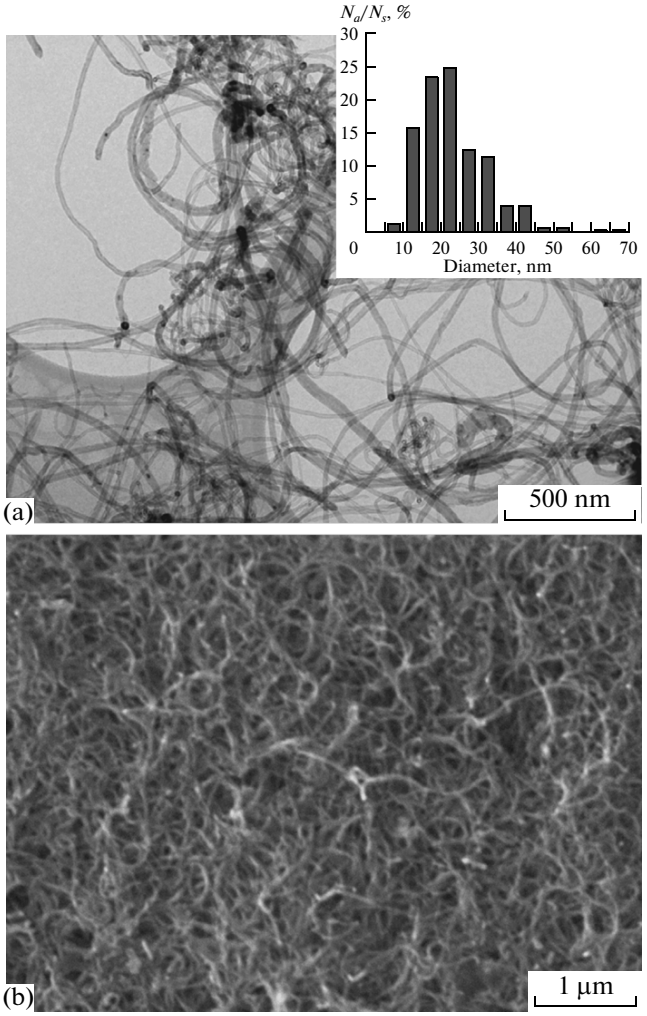

Fig. 1. (a) Electron-microscopic images of MWCNTs (20–22) ± 8 nm in diameter (JEM-2010 transmission electron microscope). (inset) Statistical diameter distribution of MWCNTs. (b) Electron-microscopic image of the paper made of MWCNTs (20–22) ± 8 nm in diameter (JSL6460LV scanning electron microscope).

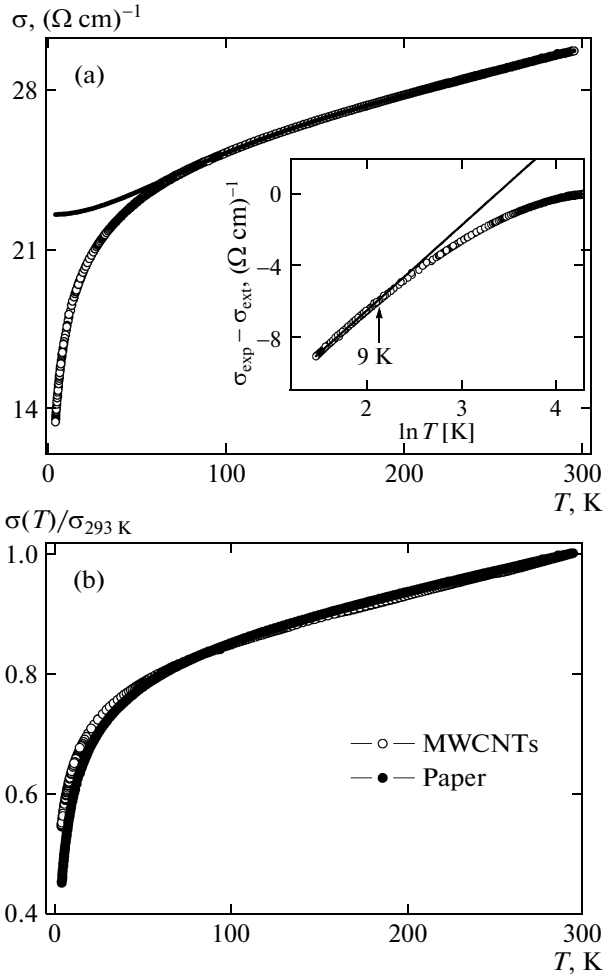

Fig. 2. (a) Temperature dependence of the electrical conductivity $\sigma(T)$ of the paper consisting of MWCNTs (20–22) ± 8 nm in diameter: (solid line) approximation of the regular part of the experimental $\sigma(T)$ data above 50 K on the assumption of its leveling off near $T = 0$ and (inset) conductivity correction for the paper $\sigma_{exp}(T) - \sigma_{ext}(T)$ vs. temperature logarithm $\ln T$. (b) Temperature dependence of normalized conductivity $\sigma(T)/\sigma_{293\,K}$ for MWCNTs (20–22) ± 8 nm in diameter and the paper made of them.

above are inappropriate to estimate the electrical resistivity of MWCNT. For example, the authors of [17, 18] achieved good contact with the surface layers of a catalytic multilayer carbonitride nanotube and found that the average resistance of the nanotube was about 50–60 kΩ/μm. Thus, the contribution of the contact to the total resistance is approximately 15–20%.

The contacts to the paper consisting of MWCNTs were made of a 0.1-mm-thick copper wire and were fixed to a 1 × 4 × 0.4-mm sample with a silver paste. Using the considerations regarding the contribution of the resistance of the contact between nanotubes, we can state that nanotubes rather than the contacts between them mainly contribute to the electrical resistivity of the paper.

Electron transport was studied with a Physical Property Measurement System (PPMS) Quantum Design device. Electrical resistivity $\rho(T)$ was measured using the four-probe method in the temperature range 4.2–295 K. Magnetoresistivity $\rho(B)$ was measured in magnetic fields up to 9 T. A magnetic field of various polarities was applied normal to the current direction. The measured magnetoresistivities were averaged over a field polarity to exclude the Hall contribution.

3. RESULTS AND DISCUSSION

Figure 2a shows the temperature dependence of the electrical conductivity of the paper consisting of MWCNTs in the temperature range 4.2–295 K. The solid line indicates the approximation of the regular part of the experimental data at $T > 50$ K on the assumption of its leveling off at temperatures near 0. An almost temperature-independent dependence of the conductivity at temperatures below 30 K is characteristic of ideal quasi-two-dimensional graphite. We now qualitatively explain the temperature dependence of the conductivity in the temperature range 0–300 K for defectless quasi-two-dimensional graphite. The valence band and the conduction band of graphite intersect each other. Let us dwell on this fact. Graphite is a semimetal (Fermi energy $E_F \sim k_B T$). The band structure of one graphite layer (graphene) represents the band structure of a zero-gap semiconductor [19]; that is, the valence band touches the conduction band. In the case of quasi-two-dimensional graphite, the interlayer interaction leads to the intersection of the conduction band and the valence band. At $T = 0$, the concentration of hole carriers in the valence band is equal to the concentration of electron carriers in the conduction band; that is, the band intersection area is half-filled. At room temperature ($T \neq 0$), electrons from the valence band pass to the conduction band; as a result, current carrier concentration n increases on scale $k_B T$ ($\Delta n/n \propto k_B T/E_F$, where Δn is the change in the carrier concentration), since $E_F \sim k_B T$. Hence, the conductivity increases according to the Drude formula ($\sigma = ne^2\tau/m$, where m is the effective mass and τ is the pulse relaxation time). At low temperatures (where $E_F \gg k_B T$, i.e., $n \gg \Delta n$), the conductivity remains constant and is related to carrier scattering by lattice defects, impurities, isotopes, and zero-point lattice vibrations.

The electronic structure of MWCNTs containing more than 20 layers is known to be similar to the structure of two-dimensional graphite. Therefore, to find the correction for the paper conductivity, we can compare our curve with the characteristic temperature dependence of the conductivity of ideal graphite obtained by the approximation of the experimental data on the paper conductivity at temperatures above 50 K. The difference between the experimental data and the approximation by the regular part is the

desired conductivity correction. The inset to Fig. 2a shows the conductivity correction in the temperature range 4.2–50 K; as the temperature decreases below 9 K, it increases logarithmically $\sigma_{exp}(T) - \sigma_{ext}(T) \sim \ln T$, where σ_{exp} is the experimental conductivity and σ_{ext} is the extrapolated conductivity. The diffuse motion of current carriers in disordered systems can occur along self-intersected trajectories, which results in quantum interference of the wavefunctions of noninteracting electrons, so-called weak localization effects. As a result, the contribution of quantum corrections, which depends on the temperature, the magnetic field, and other corrections, is added to the classical conductivity determined by the Drude formula. In a two-dimensional case, the weak localization effects depend logarithmically on temperature [21]. Hence, the experimental temperature dependence of the conductivity of the paper consisting of MWCNTs is characterized by two-dimensional quantum corrections below 9 K. This finding is also explained by the fact that, as the temperature decreases, the quantum correction lengths increase as

$$L_T = \left(\frac{\hbar D}{k_B T}\right)^{1/2}, \quad L_\varphi = (D\tau_\varphi)^{1/2},$$

$$\tau_\varphi \sim \text{const}\, T^{-p},$$

where D is the diffusion coefficient and τ_φ is the wavefunction phase breakdown time of conduction electrons. If these quantum corrections become larger than one characteristic size of the system, they are taken to be two-dimensional corrections. In our case, this parameter is the interlayer distance (0.344 nm for MWCNTs), and the wavefunction phase breakdown length of conduction electrons at 7 K ($L_\varphi \approx 13.5$ nm) is larger (the value of L_φ was taken from an analysis of the dependence of the paper magnetoresistivity given below).

The temperature dependence of the initial MWCNTs $\sigma(T)$ is similar to the dependence of the paper. The initial MWCNTs also exhibit two-dimensional quantum corrections to the conductivity at temperatures below 20 K. The temperature dependence of the initial MWCNTs is given in our work [22]. If the temperature dependences $\sigma(T)$ of MWCNTs and the related paper are normalized by the conductivity at room temperature $\sigma_{293\,K}$, the slopes of the curves in the temperature range 100–293 K coincide (Fig 2b). At the same change in $k_B T$, the slope according to the Drude formula characterizes carrier concentration n_0 at $T = 0$. This means that carrier concentrations n_0 of the initial MWCNTs and the related paper are the same. It should be noted that the amplitude of the quantum corrections to the temperature dependence of the paper is higher than the amplitude of the corrections for the initial nanotubes by about 10% (Fig. 2b).

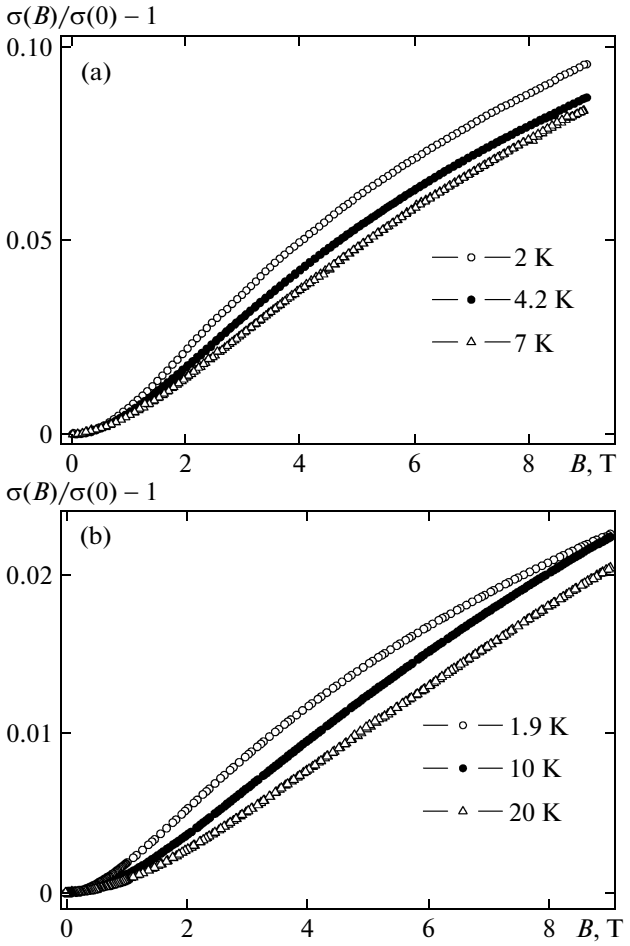

Fig. 3. Conductivity correction $\sigma(B)/\sigma(0) - 1$ vs. magnetic field B at various temperatures for (a) paper and (b) MWCNTs (20–22) ± 8 nm in diameter.

Figure 3 shows the dependence of the correction to relative conductivity $\sigma(B)/\sigma(0)$ on magnetic field B at various temperatures for catalytic MWCNTs and the related paper. The field dependence $\sigma(B)$ of the weak localization effects is caused by the suppression of the quantum corrections in a magnetic field. When a magnetic field is applied, the number of the interferences of the wavefunctions of conduction electrons decreases, and conductivity dependence $\sigma(B)$ is positive. The correction amplitude for the paper is higher (Fig. 3), since the contribution of the quantum corrections to the temperature dependence of the paper is higher than that for the initial MWCNT powders. The experimental data in Fig. 3 were approximated using the following expression for the quantum corrections of the weak localization effects to the magnetoconductivity in the two-dimensional case [23]:

$$\Delta\sigma^{WL}(B) = \frac{e^2}{2\pi^2\hbar} Y\left(\frac{4eDB}{\hbar c}\tau_\varphi\right),$$

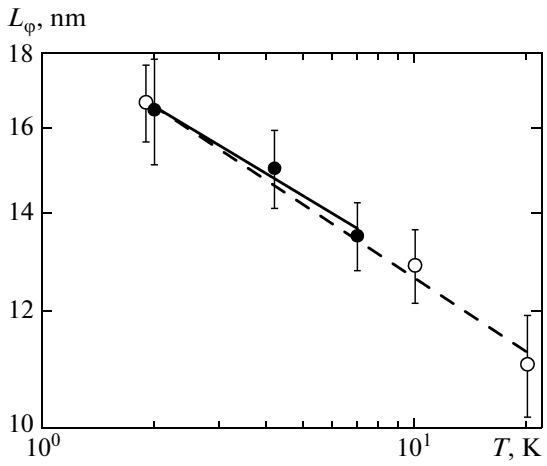

Fig. 4. Temperature dependence of the phase breakdown length $L_\varphi(T)$ for (solid circles) paper and (open circles) MWCNTs (20–22) ± 8 nm in diameter. (solid line) Approximation $L_\varphi(T) \sim T^{-P/2}$ for the paper, $P = 0.305 \pm 0.044$; (dashed line) approximation $L_\varphi(T)$ for MWCNTs, $P = 0.335 \pm 0.027$.

where

$$\Delta\sigma(B) = \sigma(B) - \sigma(B = 0),$$
$$Y(x) = \ln x + \psi(1/2 + 1/x),$$

and $\psi(y)$ is the logarithmic derivative of the Euler gamma function. Before this approximation, the values of function $Y(x)$ were calculated by a numerical method in the Maple software environment. The obtained numerical values were approximated in the Origin software environment by polynomials of various degrees. The experimental data were then processed using the obtained polynomial dependence with two parameters. The first parameter included the factor before function $Y(x)$. The second parameter is $4eD\tau_\varphi/\hbar c$ and completely enters into phase breakdown length $L_\varphi = (D\tau_\varphi)^{1/2}$. Thus, we obtain phase breakdown length L_φ at a given temperature by varying two parameters and comparing the calculated dependence $\Delta\sigma^{WL}(B)$ and the obtained experimental data (Fig. 3). The result of this approximation, namely, the temperature dependence of the phase breakdown length $L_\varphi(T)$ is shown in Fig. 4. The solid line in Fig. 4 illustrates the approximation $L_\varphi(T) = \text{const}\, T^{-P/2}$. We have $P = 0.335 \pm 0.027$ for MWCNTs and $P = 0.305 \pm 0.044$ for the paper consisting of MWCNTs. Thus, we have $P \approx 1/3$ for our samples. If changes in the wavefunction phase are related to inelastic electron scattering, we have $P = 2/3$ in the one-dimensional case and $P = 1$ in the two-dimensional case. For our materials, the temperature dependence of the phase breakdown length is much weaker, $L_\varphi \sim (T^{-1/3})^{1/2}$. The authors of [24] obtained a comparable result, namely, $P = 0.36 \pm 0.07$, when studying the magnetoresistance of individual strongly imperfect MWCNTs. They assumed that this weak temperature dependence of the phase breakdown length $L_\varphi(T)$ is related to the approach of a strong localization mode, where the theoretical model used in this work begins to describe the experimental results inadequately. Strong localization can appear due to the fact that, as the authors of [24], we use more imperfect catalytic MWCNTs as compared to electric-arc MWCNTs, which are synthesized at a higher temperature.

4. CONCLUSIONS

We studied the electrophysical properties of catalytic MWCNTs (20–22) ± 8 nm in diameter without impurities of other carbon phases and the paper made of them. The temperature dependences of the electrical conductivities of MWCNTs and the paper consisting of them exhibit the contribution of two-dimensional quantum corrections to these conductivities at a temperature below 10–15 K. As is predicted by the theory of quantum corrections, the correction to the electrical conductivity in the two-dimensional case depends logarithmically on temperature, which is caused by weak localization effects. The current carrier concentrations in the initial MWCNTs and the related paper are the same. In terms of the weak localization effects, the approximation of the contribution to the magnetoconductivity of MWCNTs or the paper based on them gives a similar temperature dependence of the phase breakdown length, $L_\varphi(T) = \text{const}\, T^{-P/2}$, where $P \approx 1/3$.

ACKNOWLEDGMENTS

The authors are grateful to A.V. Ishchenko and N.A. Rudina who obtained electron-microscopic images of MWCNTs and paper based on them, as well as to A.N. Lavrov and A.I. Romanenko for fruitful discussions of the results. This work was supported by the Russian Foundation for Basic Research (project no. 12-02-90817-mol_rf_nr), the Program of the Basic Research of the Presidium of the Russian Academy of Sciences (project no. 24.46) and integrated project no. 36 of the Siberian Branch of the Russian Academy of Sciences.

REFERENCES

1. *Carbon Nanotechnology: Recent Developments in Chemistry, Physics, Materials Science, and Device Applications*, Ed. by L. Dai (Elsevier, Amsterdam, The Netherlands, 2006).
2. A. I. Oliva-Avile's, F. Avile's, and V. Sosa, Carbon **49**, 2989 (2011).
3. W. Bai, D. Zhuo, X. Xiao, J. Xie, and J. Lin, Polym. Compos. **33** (5), 711 (2012).
4. A. E. Aliev, A. A. Fridman, and P. K. Khabibullaev, J. Commun. Technol. Electron. **50**, 1074 (2005).

5. T. Saotome, H. Kim, Z. Wang, D. Lashmore, and H. T. Hahn, Bull. Mater. Sci. **34** (4), 623 (2011).
6. L. Petrik, P. Ndungu, and E. Iwuoha, Nanoscale Res. Lett. **5**, 38 (2010)
7. H.-R. Lin, H.-Y. Miao, J.-H. Liu, C.-W. Lin, and J. Gong, Procedia Eng. **36**, 589 (2012).
8. B. Bourlon, C. Miko, L. Forró, D. C. Glattli, and A. Bachtold, Phys. Rev. Lett. **93** (17), 176806-1 (2004).
9. S.-H. Jhi, S. G. Louie, and M. L. Cohen, Solid State Commun. **123**, 495 (2002).
10. H. Dai, E. W. Wong, and C. M. Lieber, Science (Washington) **272**, 523 (1996).
11. T. W. Ebbesen, H. J. Lezec, H. Hiura, J. W. Bennett, H. F. Ghaemi, and T. Thio, Nature (London) **382** (6586), 54 (1996).
12. D. L. Carroll, Ph. Redlich, X. Blase, J.-C. Charlier, S. Curran, P. M. Ajayan, S. Roth, and M. Rühle, Phys. Rev. Lett. **81** (11), 2332 (1998).
13. C. C. Lan, P. Srisungsitthisunti, P. B. Amama, T. S. Fisher, X. Xu, and R. G. Reifenberger, Nanotechnology **19** (12), 125703-1 (2008).
14. H. J. Li, W. G. Lu, J. J. Li, X. D. Bai, and C. Z. Gu, Phys. Rev. Lett. **95** (8), 086601-1 (2005).
15. F. Wakaya, K. Katayama, and K. Gamo, Microelectron. Eng. **67–68**, 853 (2003).
16. I. Takesue, J. Haruyama, N. Kobayashi, S. Chiashi, S. Maruyama, T. Sugai, and H. Shinohara, Microelectron. J. **39** (2), 165 (2008).
17. S. Dohn, K. Molhave, and P. Boggild, Sens. Lett. **3**, 300 (2005).
18. F. Bussolotti, L. D'Ortenzi, V. Grossi, L. Lozzi, S. Santucci, and M. Passacantando, Phys. Rev. B: Condens. Matter **76** (12), 125415-1 (2007).
19. P. R. Wallace, Phys. Rev. **71**, 622 (1947).
20. A. S. Kotosonov and V. V. Atrazhev, JETP Lett. **72** (2), 53 (2000).
21. E. Abrahams, P. W. Anderson, D. C. Licciardello, and T. V. Ramakrishnan, Phys. Rev. Lett. **42** (10), 673 (1979).
22. E. N. Tkachev, A. I. Romanenko, O. B. Anikeeva, T. I. Buryakov, V. E. Fedorov, A. S. Nazarov, V. G. Makotchenko, V. L. Kuznetsov, and A. N. Usol'tseva, JETP **105** (1), 233 (2007).
23. B. L. Al'tshuler, A. G. Aronov, A. I. Larkin, and D. E. Khmel'nitskii, Sov. Phys. JETP **54** (2), 411 (1981).
24. R. Tarkiainen, M. Ahlskog, A. Zyuzin, P. Hakonen, and M. Paalanen, Phys. Rev. B: Condens. Matter **69** (3), 033402-1 (2004).

Translated by K. Shakhlevich